ORIGINAL PAPER

EFFECT OF COLD ELECTRON BEAM ON OBLIQUE PROPAGATING RELATIVISTIC EMEC WAVES FOR KAPPA DISTRIBUTION FUNCTION WITH AC FIELD FOR MAGNETO-PLASMA

R. S. PANDEY[1], RAJBIR KAUR[1], K.M. SINGH[2], VIJAY PRASAD[2], B.N. SINGH[2]

Manuscript received: 02.12.2014; Accepted paper: 18.12.2014;

Published online: 30.12.2014.

Abstract. *The effect of cold electron beam on oblique propagating electromagnetic electron cyclotron (EMEC) wave has been studied by using the unperturbed Lorentzian (Kappa) distribution in the magnetosphere for relativistic plasma. The dispersion relation is obtained following the method of characteristic solutions and kinetic approach. An expression for the growth rate of a system has been calculated. It is inferred that in addition to the relativistic plasma obliquity and effect of cold electron beam modifies the growth rate and it also shifts the wave band significantly. The relativistic electrons by increasing the growth rate and widening the bandwidth may explain a wide frequency range of EMEC wave emissions in the magnetosphere.*

Keywords: *Electron cyclotron waves, Kappa distribution, Magnetosphere*

1. INTRODUCTION

Wave particle interactions play an essential role in the formation of the magnetopause boundary layer, precipitation of energetic charged particles leading to auroras and generation of VLF emissions. The charged particles in the ionosphere and magnetosphere exhibit anisotropic distribution in momentum space, which is suitable for cyclotron instability leading to wave-growth and hence to particle precipitation into the atmosphere. Therefore, there is continuous loss of particles from the ionosphere and magnetosphere. This loss is compensated by the injection of particles at different radial distances and latitudes via slow processes such as radial convection, discussion and azimuthally drifts. During geomagnetic storm and substorm, the transfer of energy from the solar wind to the magnetosphere is significantly enhanced. The effects include dramatic changes and intensification of the particle population, the magnetic and electric fields and the electric currents in the ionosphere and magnetosphere, as well as Joule heating of the upper atmosphere. In addition, we also associate magnetic storms with the fast and large fluctuations of the electric and magnetic fields. The generation of the field aligned currents, electric fields, injection of particles, enhancement of ring current and modify the generation processes of VLF emissions and as a result emission activity is intensified during magnetic disturbances etc.

In the plasma physics the beam instabilities have been subjected to relevance for many fields. The relativistic electron beam is a special case that is especially relevant to the

[1] Affiliation 1 (Department of Physics, Amity Institute of Applied Sciences, Amity University, Sector 125, Noida, U.P, India). E-mail: rkaur2@amity.edu

[2] Affiliation 2 (Department of Physics, Veer Kunwar Singh University, Arrah, Bihar, India). E-mail: rspandey@amity.edu

relativistic flows of astrophysical plasmas, in particular the relativistic jets of micro quasars [1] gamma ray burst production scenarios [2] or the fast ignition scenario [3] in inertial confinement fusion or to or pulsar winds [4]. Due to the analytical complexity of the electromagnetic dispersion equation involved, these oblique modes were first investigated in the fluid approximation [5-6]. In recent past, the temperature-dependent model based on kinetic theory [Bret et al. 2005] shows that a cold fluid model recovers a continuum of most unstable modes, whereas the most unstable mode of the system has been quite localized in the **k** space [8]. Furthermore, the kinetic model confirms a particular orientation of the wave vector relative to the beam velocity vector for which the instability domain is unbounded [9-10]. There are numerous physical situations involving magnetized plasma, especially in astrophysics. Regarding oblique unstable modes, Godfrey *et al.* [11] have shown with the help of a fluid approximation that their growth rates are significantly reduced by a magnetic field in the case of a cold beam and a cold plasma. Therefore, the growth of oblique modes cannot be fully suppressed. It was concluded that temperature and magnetic field are important for the growth of oblique waves. Thermal effects localize the maximum growth rate on one single wave vector and prompt an oblique critical direction and high values for the unstable **k**. The introduction of a parallel static magnetic field changes the spectrum of oblique instabilities and reduces their growth rates. Therefore, it seems beneficial to investigate the interplay of both effects and more specifically, to assess their joint effect on the growth rate map. Two-stream unstable modes **k** parallel to the beam are electrostatic, whereas filamentation modes are purely transverse. Nevertheless, both instabilities pertain to the same branch of the dispersion equation and as a function of the angle between the wave vector and the beam velocity vector, it enclose a continuum of unstable modes [12]. These intermediate modes are, neither purely electrostatic nor purely transverse, therefore, a fully electromagnetic formalism is mandatory to refer to them. If we also wish to study temperature and magnetic field effects, the kinetic formalism becomes hardly tractable for oblique modes analytically, however some very interesting kinetic treatments of the magnetized case are available for the instability [13] and the two stream one [14-15]. Bret and Deutsch [16] has described the main effects of a finite temperature on the oblique modes.

Electric field measurements at magnetospheric heights and shock region have given values of AC field along and perpendicular to Earth's magnetic field [17-19]. Various authors have discussed the role of parallel DC and AC electric fields on the whistler mode instability in the magnetosphere generally adopting plasma dispersion function which is based on anisotropic Maxwellian distributions to describe the resonant population [20-21].

In the present paper the velocity of background plasma has been considered in the order of velocity of light, so the relativistic approach of mass changing with velocity has been taken in account. At the same time other authors have not incorporated the analytical study in detail. In the present paper giving the analytical treatment in detail the effect of cold plasma beam on oblique electromagnetic EMEC wave with perpendicular AC electric field has been studied by using the unperturbed Lorentzian (Kappa) distribution in the Earth's atmosphere for relativistic plasma. The cold plasma has been described by a simple Maxwellian distribution where as Lorentzian (Kappa) distribution function has been derived for relativistic plasma with temperature anisotropy in the presence of a perpendicular AC electric field to form a hot/warm background. The dispersion relation is obtained by using the method of characteristic solutions and kinetic approach. An expression for the growth rate of a system with added cold plasma injection has been calculated. Results for representative values of parameters suited to the Earth's magnetosphere have been obtained. It is inferred that in addition to the relativistic plasma obliquity and effect of cold electron beam modifies the growth rate and it also shifts the wave band significantly. The relativistic electrons by increasing the growth rate and widening the bandwidth may explain a wide frequency range

of EMEC wave emissions in the magnetosphere. The salient features of the analysis and the results obtained have been discussed.

2. MATHEMATICAL FORMULATIONS

A spatially homogeneous anisotropic, collision-less relativistic plasma subjected to external magnetic field $\mathbf{B_o} = B_o\hat{\mathbf{e}}_\mathbf{z}$ and an electric field $\mathbf{E_o} = E_o \sin(\upsilon t)\hat{\mathbf{e}}_\mathbf{x}$ has been considered to get dispersion relation. In this case, linearized Vlasov-Maxwell equations, obtained after neglecting higher order terms and separating the equilibrium and non-equilibrium parts, following the technique of Pandey et al. [22] is given as below:

$$\mathbf{v}.\left(\frac{\partial f_{so}}{\partial \mathbf{r}}\right) + \frac{e_s}{m_s}\left[E_o \sin(\upsilon t) + \left(\frac{\mathbf{v}\times\mathbf{B_o}}{c}\right)\right]\left(\frac{\partial f_{so}}{\partial \mathbf{v}}\right) = 0 \tag{1}$$

$$\frac{\partial f_{s1}}{\partial t} + \mathbf{v}.\left(\frac{\partial f_{s1}}{\partial \mathbf{r}}\right) + \left(F/m_s\right)\frac{\partial f_{s1}}{\partial \mathbf{v}} = S(\mathbf{r},\mathbf{v},t) \tag{2}$$

where force is given as $F = m\dfrac{dv}{dt}$

$$\mathbf{F} = e_s\left[E_o \sin(\upsilon t) + \left(\frac{\mathbf{v}\times\mathbf{B_o}}{c}\right)\right] \tag{3}$$

The particle trajectories are obtained by solving equation of motion defined in equation (3) and S(r,v,t) is defined as:

$$S(\mathbf{r},\mathbf{v},t) = -(e/m_s)\left[E_1 + \left(\frac{\mathbf{v}\times\mathbf{B_1}}{c}\right)\right]\left(\frac{\partial f_{so}}{\partial \mathbf{v}}\right) \tag{4}$$

where s denotes species and E_1, B_1 and f_{s1} are perturbed quantities and are assumed to have harmonic dependence in E_1, B_1 and f_{s1}=exp i(**k.r**− ωt). The method of characteristic solution is used to determine the perturbed distribution function, fs_1, which is obtained from Eq. (2) by

$$f_{s1}(\mathbf{r},\mathbf{v},t) = \int_0^\infty s\{\mathbf{r_o}(\mathbf{r},\mathbf{v},t'), \mathbf{v_o}(\mathbf{r},\mathbf{v},t'), t-t'\}dt' \tag{5}$$

The phase space coordinate system has been transformed from $(\mathbf{r},\mathbf{v},t)$ to $(\mathbf{r_o},\mathbf{v_o},t-t')$. The particle trajectories which are obtained by solving eq. (3) for the given external field and wave propagation, $\mathbf{k} = \left[k_\perp \hat{e}_x, 0, \mathbf{k}_\parallel \hat{e}_z\right]$ are:

$$X_0 = X + \left(\frac{P_\perp \sin\theta}{\omega_{cs} m_s}\right) - \left[P_\perp \sin\left\{\frac{\theta + \left(\frac{\omega_{cs} t}{\gamma}\right)}{\omega_{cs} m_s}\right\}\right] + \left[\frac{\Gamma_{xs} \sin \upsilon t}{\gamma\left\{\left(\frac{\omega_{cs}}{\gamma}\right)^2 - \upsilon^2\right\}}\right] - \left[\frac{\upsilon \Gamma_{xs} \sin\left(\frac{\omega_{cs} t}{\gamma}\right)}{\omega_{cs}\left\{\left(\frac{\omega_{cs}}{\gamma}\right)^2 - \upsilon^2\right\}}\right]$$

$$Y_0 = Y - \left(\frac{P_\perp \cos\theta}{\omega_{cs} m_s}\right) + \left[P_\perp \cos\left\{\frac{\theta + \left(\frac{\omega_{cs} t}{\gamma}\right)}{\omega_{cs} m_s}\right\}\right] + \left(\frac{\Gamma_{xs}}{\upsilon \omega_{cs}}\right) - \frac{\left\{1 + \upsilon^2 \beta^2 \cos\left(\frac{\omega_{cs} t}{\gamma}\right) - \omega_{cs}^2 \cos \upsilon t\right\}}{\gamma^2\left\{\left(\frac{\omega_{cs}}{\gamma}\right)^2 - \upsilon^2\right\}}$$

$$z_0 = z - \frac{P_z}{\lambda m_s} \tag{6}$$

and the velocities are

$$v_{xo} = P_\perp \cos\left\{\theta + \frac{\left(\frac{\omega_{cs} t}{\gamma}\right)}{\gamma m_s}\right\} + \left[\frac{\upsilon \Gamma_{xs}}{\gamma\left\{\left(\frac{\omega_{cs}}{\gamma}\right)^2 - \upsilon^2\right\}}\right]\left\{\cos \upsilon t - \cos\left(\frac{\omega_{cs} t}{\gamma}\right)\right\}$$

$$v_{yo} = P_\perp \sin\left\{\theta + \frac{\left(\frac{\omega_{cs} t}{\gamma}\right)}{\gamma m_s}\right\} + \left[\frac{\Gamma_x}{\gamma\left\{\left(\frac{\omega_{cs}}{\gamma}\right)^2 - \upsilon^2\right\}}\right]\left\{\left(\frac{\omega_{cs}}{\gamma}\right)\sin \upsilon t - \upsilon \sin\left(\frac{\omega_{cs} t}{\gamma}\right)\right\} \tag{7}$$

$$v_{zo} = \frac{P_z}{\gamma m_s}, v_x = \frac{P_\perp \cos\theta}{\gamma m_s} \quad , \quad v_y = \frac{P_\perp \sin\theta}{\gamma m_s}, \quad v_z = \frac{P_z}{\gamma m_s}$$

$$m_s = \frac{m_{0s}}{\gamma}, \quad \omega_{cs} = \frac{e_s B_0}{m_s} \; \gamma = \sqrt{1 - \frac{v^2}{c^2}}, \Gamma_{xs} = \frac{e_s E_o}{m_s}$$

$P_\perp$ and P_z denote momenta perpendicular and parallel to the magnetic field. Using equations (5), (6) and the Bessel identity and performing the time integration, following the technique and method of Pandey and Kaur [23], the perturbed distribution function is found after some lengthy algebraic simplifications as :

$$f_{s1} = -\left(\frac{ie_s}{m_s \gamma \omega}\right)\sum J_s(\lambda_3)\exp(i(m-n)\theta)\left[\frac{J_m J_n J_p U^* E_{1x} - iJ_m V^* E_{1y} + J_m J_n J_p W^*}{\omega - \left(\frac{k_\parallel P_z}{\gamma m_s} + p\upsilon - \frac{(n+g)\omega_{cs}}{\gamma}\right)}\right]$$

Due to the phase factor the solution is possible when m = n. Here

$$U^{*}=\left(\frac{c_1P_{\perp}n}{\gamma\lambda_1m_s}\right)-\left(\frac{n\upsilon c_1D}{\lambda_1}\right)+\left(\frac{p\upsilon c_1D}{\lambda_2}\right),\ V^{*}=\left(\frac{c_1P_{\perp}J_nJ_p}{\gamma m_s}\right)+c_1DJ_pJ_n\omega_{cs}$$

$$W^{*}=\left(\frac{n\omega_{cs}Fm_s}{k_{\perp}P_{\perp}}\right)+\left(\gamma m_sP_{\perp}\omega\frac{\partial f_0}{\partial P_z}\right)+G\left\{\left(\frac{p}{\lambda_2}\right)-\left(\frac{n}{\lambda_1}\right)\right\}$$

$$C_1=\left\{\frac{(\gamma m_s)}{P_{\perp}}\right\}\left(\frac{\partial f_0}{\partial P_{\perp}}\right)\left(\omega-\frac{k_{\parallel}p_z}{\gamma m_s}\right)+k_{\parallel}\gamma m_s\left(\frac{\partial f_0}{\partial P_{\perp}}\right) \tag{8}$$

$$D=\frac{\Gamma_{xs}}{\gamma\left\{\left(\frac{\omega_{cs}}{\gamma}\right)^2-\upsilon^2\right\}},\ F=\frac{Hk_{\perp}P_{\perp}}{\gamma m_s},\ H=\left\{\frac{(\gamma m_s)^2}{P_{\perp}}\right\}\left(\frac{\partial f_0}{\partial P_{\perp}}\right)\left(\frac{P_z}{\gamma m_s}\right)+\gamma m_s\left(\frac{\partial f_0}{\partial P_z}\right)$$

$$G=\frac{Hk_{\perp}\upsilon\Gamma_{xs}}{\gamma\left\{\left(\frac{\omega_{cs}}{\gamma}\right)^2-\upsilon^2\right\}},\quad J_n(\lambda_1)=\frac{dJ_n(\lambda_1)}{d\lambda_1},\ J_p(\lambda_2)=\frac{dJ_p(\lambda_2)}{d\lambda_2}$$

and the Bessel function arguments are defined as

$$\lambda_1=\frac{k_{\perp}P_{\perp}}{\omega_{cs}m_s},\quad \lambda_3=\frac{k_{\perp}\upsilon\Gamma_{xs}}{\gamma\left\{\left(\frac{\omega_{cs}}{\gamma}\right)^2-\upsilon^2\right\}}\quad \lambda_2=\frac{k_{\perp}\Gamma_{xs}}{\gamma\left\{\left(\frac{\omega_{cs}}{\gamma}\right)^2-\upsilon^2\right\}}$$

The conductivity tensor is written as

$$\|\sigma\|=\frac{-i\sum\left(e_s^2/m_s\lambda\right)^2\omega\int d^3PJ_g(\lambda_3)\|s\|}{\left[\omega-\left(\frac{k_{\parallel}P_z}{\gamma m_s}\right)-\left((n+g)\frac{\omega_{cs}}{\gamma}\right)+p\upsilon\right]} \tag{9}$$

where

$$\|S\|=\begin{vmatrix} P_{\perp}J_n^2J_p\left(\frac{n}{\lambda_1}\right)U^{*} & iP_{\perp}J_nV^{*} & P_{\perp}J_n^2J_p\left(\frac{n}{\lambda_1}\right)W^{*}\\ iP_{\perp}J_n'J_nJ_p\left(\frac{n}{\lambda_1}\right)U^{*} & P_{\perp}J_n'V^{*} & iP_{\perp}J_n'J_nJ_p\left(\frac{n}{\lambda_1}\right)W^{*}\\ P_zJ_n^2J_p\left(\frac{n}{\lambda_1}\right)U^{*} & iP_zJ_nV^{*} & P_zJ_n^2J_p\left(\frac{n}{\lambda_1}\right)W^{*}\end{vmatrix} \tag{10}$$

By using these in the Maxwell's equations we get the dielectric tensor,

$$\varepsilon_{ij} = 1 + \sum\left\{\frac{4\pi e_s^2}{(\gamma m_s)^2 \omega}\right\}\int \frac{d^3 P J g(\lambda_3) \| S \|}{\left(\omega - \frac{k_\| P_z}{\gamma m_s}\right) - \left\{\frac{(n+g)\omega_{cs}}{\gamma}\right\} + p\upsilon} \tag{11}$$

The generalized dielectric tensor may be written as:

$$\begin{vmatrix} N^2\cos^2\theta_1 + \varepsilon_{11} & \varepsilon_{12} & N^2\cos\theta_1\sin\theta_1 + \varepsilon_{13} \\ \varepsilon_{21} & N^2 + \varepsilon_{22} & \varepsilon_{23} \\ N^2\cos\theta_1\sin\theta_1 + \varepsilon_{31} & \varepsilon_{32} & N^2\sin^2\theta_1 + \varepsilon_{33} \end{vmatrix} \tag{12}$$

After using the limits in above tensor $\mathbf{k}_\perp = k\sin\theta_1 \to 0$ and $\mathbf{k}_\| = k\cos\theta_1$, the generalized dielectric tensor becomes simplified tensor:

$$\begin{vmatrix} -N^2 + \varepsilon_{11} & \varepsilon_{12} & 0 \\ -\varepsilon_{21} & -N^2 + \varepsilon_{22} & 0 \\ 0 & 0 & \varepsilon_{33} \end{vmatrix} \tag{13}$$

For EMEC waves, it is rewritten in more convenient form:

$$-N^4 - 2\varepsilon_{11}N^2 + \varepsilon_{11}^2 + \varepsilon_{12}^2 = 0 \tag{14}$$

Neglecting the higher order terms of N, the relation becomes:

$$\varepsilon_{11} \pm \varepsilon_{12} = N^2 \tag{15}$$

where N is index of refraction.

The unperturbed Lorentzian-Kappa distribution function is:

$$F_{ok} = \frac{n_o}{\pi^{3/2}\theta_1^2\boldsymbol{\theta}_\| k^{3/2}} \frac{\Gamma(k+1)}{\Gamma(k+1/2)}\left[1 + \frac{\mathbf{v}_\|^2}{k\boldsymbol{\theta}_\|^2} + \frac{\mathbf{v}_\perp^2}{k\boldsymbol{\theta}_\perp^2}\right]^{-(k+1)} \tag{16}$$

and associated parallel and perpendicular effective thermal speeds are

$$\boldsymbol{\theta}_\| = \left[\frac{2k-3}{k}\right]^{1/2}\left(\frac{T_\|}{m_s}\right)^{1/2}, \qquad \boldsymbol{\theta}_\perp = \left[\frac{2k-3}{k}\right]^{1/2}\left(\frac{T_\perp}{m_s}\right)^{1/2}$$

Applying the approximation of electron-cyclotron range of frequencies has been done. In this case, ion temperature are assumed $T_{is} = T_{i\|} = T_i$ and assumed to be magnetized with $|\omega_r + i\gamma| << \omega_{cs}$ while electrons are assumed to have $T_{\perp e} > T_{\|e}$ and

$|k_{\|}\alpha_{\|}| << |\omega_r \pm \omega_{cs} + i.\gamma|$ for background plasma. Therefore Equation (11) becomes the following, as a sum of background and injected cold beam plasma:

$$D(k,\omega_r+i\gamma)=1-\frac{k^2c^2}{\omega_r+i\gamma}+\sum\frac{J_p(\lambda_2)J_q(\lambda_3)}{\alpha_{\perp s}^2}\left[\left\{\frac{\omega_i^2}{\omega_{ce}^2}-\frac{\omega_{pi}^2}{(\omega_r+i\gamma)\pm\omega_{ce}}\right\}\left\{X_1 i\frac{\omega_{pi}^2}{(\omega_r+i\gamma)}\right\}\frac{\omega_r+i\gamma}{k_{\|}\theta_{\|e}}\left(\frac{k-1}{k}\right)^{1/2}\right]\times$$

$$\left[\left(\frac{k-1}{k-3/2}\right)Z_{k-1}\left(\left(\frac{k-1}{k}\right)1/2\xi_e\right)A_T\left\{1+\xi_e\left(\left(\frac{k-1}{k}\right)^{1/2}\left(\frac{k-1}{k-3/2}\right)Z_{k-1}^{*}\left(\frac{k-1}{k}\right)^{1/2}\xi_e\right)\right\}\right]-\frac{\omega}{\omega\pm\omega_c}\frac{\omega_{pc}^2}{\omega_{pw}^2}\quad(17)$$

where

$$X_{1i}=\theta_{\perp i}^2-\frac{\upsilon\Gamma_{xi}}{\omega_{ci}^2-\upsilon^2}\frac{\theta_{\perp i}}{2}\sqrt{\pi}$$

$$X_{1e}=\theta_{\perp e}^2-\frac{\upsilon\Gamma_{xe}}{\omega_{ce}^2-\upsilon^2}\frac{\theta_{\perp e}}{2}\sqrt{\pi}$$

$$A_T=\frac{\theta_{\perp e}^2}{\theta_{\|e}^2}-1$$

$Z(\xi)=$ Plasma Dispersion Function

here the function $Z_{\kappa-1}^{*}$ occurring in Eq. (17) is the modified plasma dispersion function defined by *Summers and Thorne*[1991].

$$Z_\kappa^*(\xi)=\frac{1}{\sqrt{\pi}}\frac{\Gamma(\kappa-1)}{\kappa^{3/2}\Gamma(\kappa-1/2)}\int_{-\infty}^{\infty}\frac{ds}{(s-\xi)\left(1+s^2/\kappa\right)^{\kappa+1}}\ldots \qquad (18)$$

$$\mathrm{Im}(\xi)>0$$

The power series $Z_\kappa^*(\xi)$ is given by

$$Z_\kappa^*(\xi)=\frac{i\kappa!\kappa^{(\kappa-1/2)}\sqrt{\pi}}{\Gamma(\kappa-1/2)\xi^{2(\kappa+1)}}\left(1-\frac{\kappa(\kappa+1)}{\xi^2}+\ldots\ldots\right)-$$

$$\left(\frac{2\kappa-1}{2\kappa}\right)\frac{1}{\xi}\left[1+\left(\frac{\kappa}{2\kappa-1}\right)\frac{1}{\xi^2}+\ldots\ldots\right]$$

For $(\xi)\longrightarrow\infty$ ...(19)

Applying condition $\frac{k^2c^2}{\omega^2} >> 1+\frac{\omega_{pi}^2}{\omega_{ci}^2}$ with p=1, n=1 and q=0 we can get the growth rate and real frequency using

$$K_3 = 1-\gamma X_3+\gamma X_4, \quad K_4 = \frac{\gamma X_3}{1-\gamma X_3+\gamma X_4}, \quad \tilde{\mathbf{k}} = \frac{\mathbf{k}_{\|}\boldsymbol{\alpha}_{\|}}{\omega_{cs}}, \qquad \beta = \frac{K_B T_{\|}\mu_o n_o}{B_o^2} \qquad \Gamma_{xs} = \frac{eE_o}{m_s}$$

$$X_4 = \frac{-\gamma\upsilon}{\omega_{ce}} \qquad \delta = 1+\frac{n_c}{n_w}(1+\gamma X_4)$$

the reduced dielectric tensor in equation (18) for EMEC waves propagate oblique to magnetic field direction is written as

$$\varepsilon_{11} \pm \varepsilon_{12} = N^2\cos^2\theta \tag{20}$$

Using equations (18), (19) and (20) in eqn (17), following the similar approach, the expression of growth rate and real frequency becomes:

$$\frac{\gamma}{\omega_{ce}} = \frac{\frac{\sqrt{\pi}}{\gamma\tilde{\mathbf{k}}\cos\theta}\left(\frac{(k-1)!\,k^{k-1/2}}{(k-3/2)!}\right)(A_T-K_4)K_3^3\left\{-\left(\frac{k^3}{\tilde{\mathbf{k}}\cos\theta}\right)\right\}^{-2k}}{1+\gamma X_4+\frac{k\cos^2\theta}{k-3/2}\left[\frac{(1+\gamma X_4)\tilde{\mathbf{k}}^2}{2K_3^2}+\frac{\tilde{\mathbf{k}}^2}{K_3}(A_T-K_4)\right]-\frac{X_{1e}}{X_{1i}}K_3^2+\frac{(\delta-1)K_3^2}{(1-X_3)^2(1+\gamma X_4)}} \tag{21}$$

$$X_3 = \frac{\omega_r}{\omega_{ce}} = \frac{\tilde{\mathbf{k}}^2\cos^2\theta}{\gamma\delta\beta}\left[\frac{X_{1e}(1+\gamma X_4)}{X_{1e}-X_{1i}(1+\gamma X_4)}+\frac{A_T\beta X_{1e}}{2(1+\gamma X_4)(X_{1e}-X_{1i}(1+\gamma X_4))}\right] \tag{22}$$

3. PLASMA PARAMETERS

To study the variation of dimensionless growth rate of oblique propagating electromagnetic electron-cyclotron waves consisting of kappa distribution function, following plasma parameters have been considered B_0 = 1x10^{-7}T, E_o = 4 mV/m, $k_B T_{\|i}$=100eV, $k_B T_{\|e}$ =5KeV, $T_\perp/T_\|$ = 1.25, 1.5, 1.75, υ = 2KHz, 3KHz, 4KHz and n_c/n_w= 10,15,20,30. When oblique propagation of EMEC waves is studied, the angle of propagation is varied too. According to this choice of plasma parameters, the discussion of the results is given as:

4. RESULTS AND DISCUSSION

Fig. 1 shows the **v**ariation of dimensionless growth rate with respect to $\tilde{k}$ for various values of temperature anisotropy, $T_\perp/T_\|$-1, and other fixed parameters as listed in figure caption.

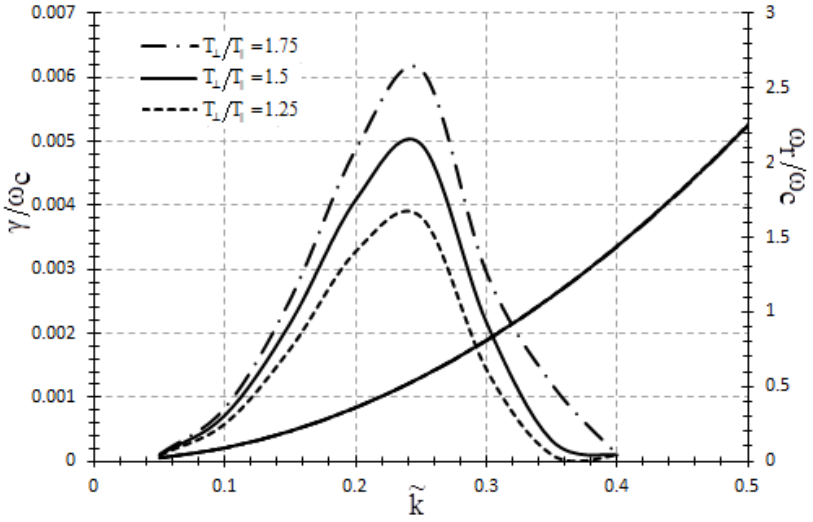

Fig 1. Variation of Growth Rate and Real Frequency with respect to $\tilde{k}$ for various values $T_\perp/T_{ll}$ at $n_c/n_w = 10$, $\gamma = 0.5$, υ=2KHz, $\theta = 10^0$ and other fixed plasma parameters.

The growth rate is 0.0039 for $T_\perp/T_{||}$=1.25 at $\tilde{k}$=0.25, the growth rate is 0.0050 when $T_\perp/T_{||}$=1.5 at $\tilde{k}$=0.26 and growth rate is γ/ω_c=0.0062 for $T_\perp/T_{||}$=1.75 at $\tilde{k}$=0.27. As the temperature anisotropy in the background plasma increases the growth rate of obliquely propagating EMEC waves, increases. Although the difference in increase of growth rate is less than compared to parallel propagation but the bandwidth increases in case of oblique propagation.

Fig. 2 shows the variations of dimensionless growth rate with respect to $\tilde{k}$ for various values of magnitude of AC frequencies at other plasma parameters being fixed and listed in the figure caption.

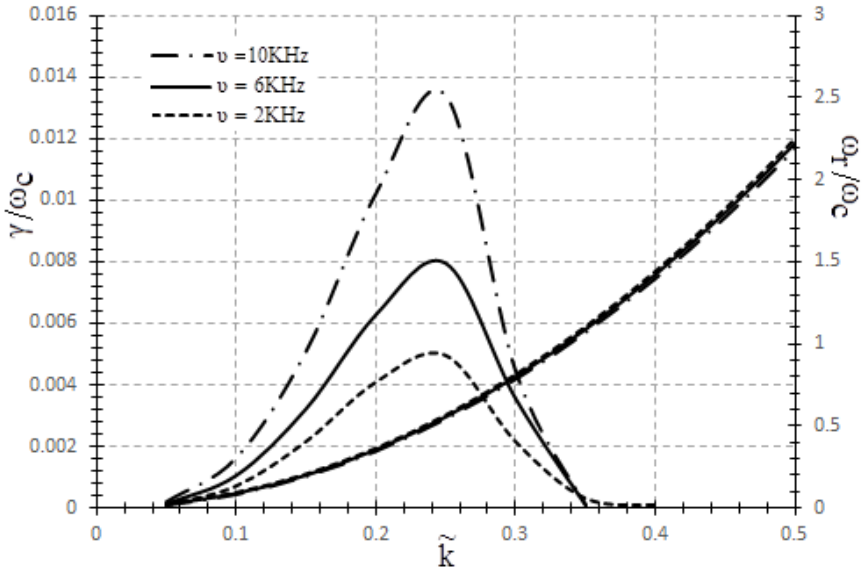

Fig 2. Variation of Growth Rate and Real Frequency with respect to $\tilde{k}$ for various values of AC frequency υ, at $T_\perp/T_{ll}$ =1.25, $\gamma = 0.5$, $\theta = 10^0$ $n_c/n_w = 10$ and other fixed plasma parameters.

The figure shows that for different values of AC frequency the peak value of growth rate appears at wave number $\tilde{k}$=0.24. For υ = 2 KHz, 3 KHz and 4KHz, growth rate is γ/ω_c = 0.00513, 0.008, 0.013 respectively. It is seen that growth rate increases with increasing value of υ.The growth rate increases with increase in value of a.c. frequency due to negative exponential of Landau damping. Also maxima shifts to lower values of $\tilde{k}$ showing that the a.c. frequency modifies resonance frequency. The perpendicularelectric field contributes significantly tothe emission of VLF signals and explains the low frequencyside of the spectrum. The modification of perpendicular velocity contributes to energy exchange between electrons, components of the wave electric field and the impressed AC field. Thus it is leading to growth or the damping of cyclotron waves.

Fig. 3 shows the **v**ariation of relativistic dimensionless growth rate with respect to $\tilde{k}$ for various angles of propagation θ, at other plasma parameters being fixed and stated in figure caption. At $\tilde{k}$= 0.25, γ/ω_c = 0.005 for θ=10^o, at $\tilde{k}$= 0.25, γ/ω_c = 0.0051 for θ=20^o and at $\tilde{k}$= 0.29, γ/ω_c = 0.0049 for θ=30^o. It is seen that growth rate decreases with increasing value of ratio of θ.

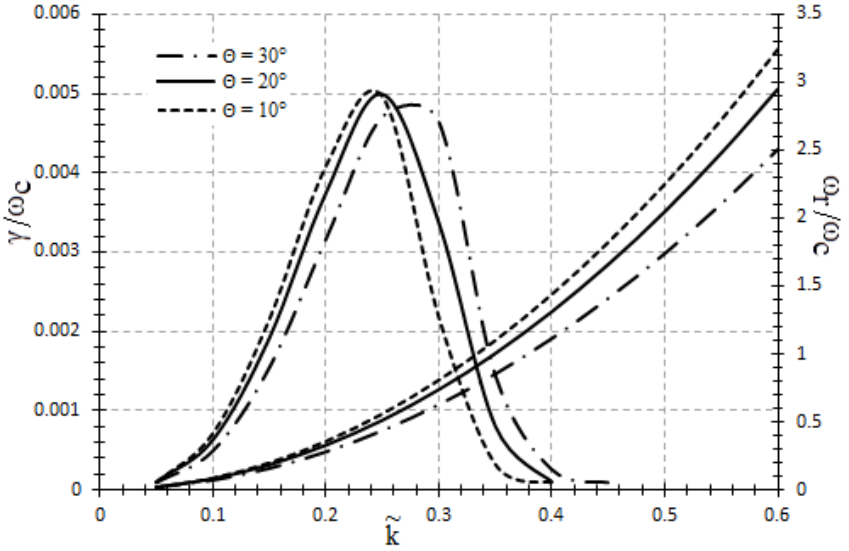

Fig 3. Variation of Growth Rate and Real Frequency with respect to $\tilde{k}$ for various values of angle of propagation θ at AC frequency $\upsilon = 2KHz$, $T_\perp/T_{ll}$ =1.25, $\gamma = 0.5$, $n_c/n_w = 10$ and other fixed plasma parameters.

This implies that growth rate increases more when waves propagate parallel to magnetic field direction that in case of oblique propagation. Study can be compared with Pandey et al. [2012].

Fig. 4 shows the **v**ariation of dimensionless growth rate with respect to $\tilde{k}$ for various values of ratio of number density of cold electrons to hot electrons. The figure explains that for n_c/n_w =10, 20 and 30, peak values occur at $\tilde{k}$=0.20, 0.28 and 0.34 respectively. For different ratio of number density the growth rate varies slightly ie. γ/ω_c = 0.00513 for n_c/n_w = 10, γ/ω_c = 0.0070 for n_c/n_w = 20 and γ/ω_c = 0.0087 for n_c/n_w = 30.

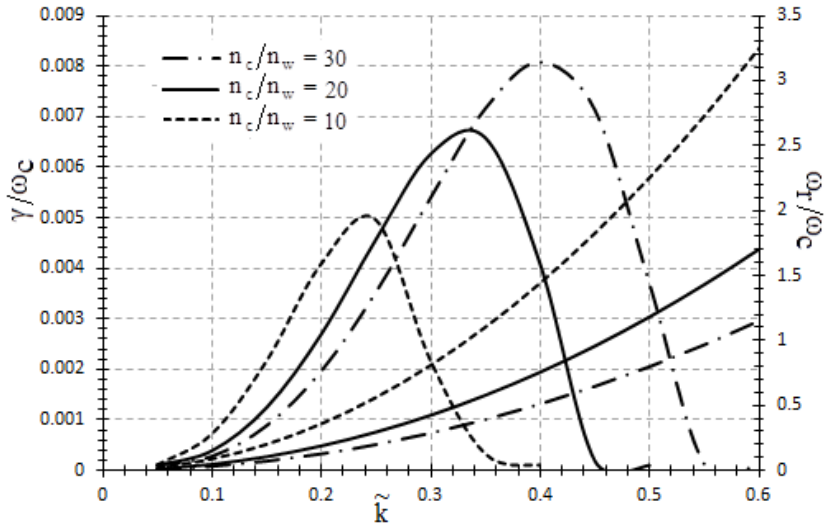

Fig 4. Variation of Growth Rate and Real Frequency with respect to $\tilde{k}$ for various values of n_c/n_w at $T_\perp/T_{ll}$ =1.25, $\gamma = 0.5$, υ=2KHz,, $\theta = 10^0$ and other fixed plasma parameters.

Second harmonic generation for higher ratio of cold to hot electrons number density can be seen in this figure. Also the bandwidth increases significantly when injection of more cold electrons is considered.

Fig. 5 shows the **v**ariation of growth rate and real frequency with respect to $\tilde{k}$ for various values of relativistic factor of background plasma and other fixed parameters as listed in figure caption.

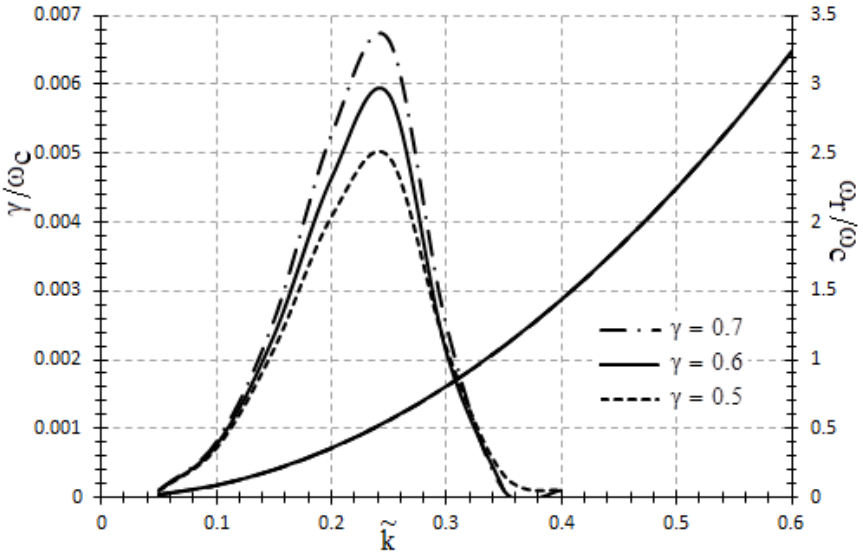

Fig 5. Variation of Growth Rate and Real Frequency with respect to $\tilde{k}$ for various values of γ at $n_c/n_w = 10$, $T_\perp/T_{ll}$ =1.25, υ=2KHz, $\theta = 10^0$ and other fixed plasma parameters.

In this graph the growth rate increases with increase of relativistic factor and maxima is fixed for $\tilde{k}$ values. It is clear from the figure that the relativistic factor is the source of energy to drive the excitation of the wave. The real frequency increases with increasing value of $\tilde{k}$. This satisfied the condition of electromagnetic waves.

REFERENCES

[1] Fender, R., Bellloni, T., *Annu. Rev. Astron. Astrophys.*, **42**, 317, 2004.
[2] Piran, T., *Rev. Mod. Phys.*, **76**, 1143, 2004.
[3] Tabak, M. et al., *Phys. Plasmas*, **1**, 1626, 1994.
[4] Y.A. Gallant and J. Arons, *Astrophys. J.*, **435**, 230, 1997.
[5] Fanberg, Y.B. et al., *Sov. Phys. JETP*, **30**, 528, 1970.
[6] Califano, F. et al., *Phys. Rev. E*, **58**, 7837, 1998.
[7] Bret, A. et al., *Phys. Rev. Lett.*, **94**, 115002, 2005.
[8] Bret, A. et al., *Phys. Rev. E*, **70**, 046401, 2004.
[9] Taguchi, T. et al., *Comput. Phys. Commun*., **164**, 269, 2004.
[10] Godfrey, B.B. et al., *Phys. Fluids*, **18**, 346, 1975.
[11] Cary, J.R. et al., *Phys. Fluids*, **24**, 1818, 1981.
[12] Tautz, R.C., Schlickeiser, R., *Phys. Plasmas*, **12**, 122901, 2005.
[13] Tautz, R.C. et al., *Phys. Plasmas*, **13**, 052112, 2006.
[14] Bret, A., Deutsch, C., *Phys. Plasmas*, **13**, 042106, 2006.
[15] Mozer, F.S. et al., *Space Sci. Rev.*, **22**, 791, 1978.
[16] Wygant, J.R. et al., *J.Geophys. Res.*, **92**, 11109, 1987.
[17] Lindquist, P.A., Mozer, F.S., *J. Geophys. Res.*, **95**, 17137, 1990.
[18] Misra, K.D., Pandey, R.S., *J. Geophys. Res.*, **100**, 19405, 1995.
[19] Misra, K.D., Singh, B.D., *J. Geophys. Res.*, **85**, 5138, 1980.
[20] Pandey, R.S. et al, *Indian Journal of Radio & Space Physics*, **34**, 98, 2005.
[21] Pandey, R.S., Kaur, R., *Progress in Electromagnetic Research M*, **45**, 337, 2012.